

Tuning the Binding Strength of Even and Uneven Hydrogen-Bonded Arrays with Remote Substituents

Stephanie C. C. van der Lubbe,[§] Anissa Haim,[§] Thor van Heesch, and Célia Fonseca Guerra*

Cite This: *J. Phys. Chem. A* 2020, 124, 9451–9463

Read Online

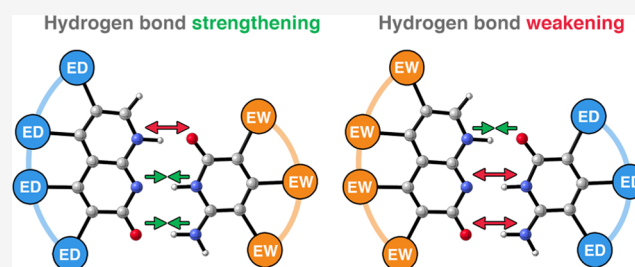
ACCESS |

Metrics & More

Article Recommendations

Supporting Information

ABSTRACT: We investigated the tunability of hydrogen bond strength by altering the charge accumulation around the frontier atoms with remote substituents. For pyridine...H₂O with NH₂ and CN substituted at different positions on pyridine, we find that the electron-withdrawing CN group decreases the negative charge accumulation around the frontier atom N, resulting in weakening of the hydrogen bond, whereas the electron-donating NH₂ group increases the charge accumulation around N, resulting in strengthening of the hydrogen bond. By applying these design principles on DDAA–AADD, DADA–ADAD, DAA–ADD, and ADA–DAD hydrogen-bonded dimers, we find that the effect of the substituent is delocalized over the whole molecular system. As a consequence, systems with an equal number of hydrogen bond donor (D) and acceptor (A) atoms are not tunable in a predictable way because of cancellation of counteracting strengthening and weakening effects. Furthermore, we show that the position of the substituent and long-range electrostatics can play an important role as well. Overall, the design principles presented in this work are suitable for monomers with an unequal number of donor and acceptor atoms and can be exploited to tune the binding strength of supramolecular building blocks.



1. INTRODUCTION

Hydrogen-bonded arrays are used as building blocks in supramolecular polymers that can be used in a wide range of applications.^{1–6} A well-known example is the 2-ureido-4-pyrimidone (UPy) monomer that was developed by Meijer et al., which forms four hydrogen bonds and can be used for the manufacturing of strong, reversible self-assembling polymer systems.^{7–10} As the properties of materials can be controlled by tuning the hydrogen bond strength,^{11–13} a design principle to control the binding strength is highly desirable.

A widely used model to predict and explain trends in hydrogen bond strengths is the secondary electrostatic interaction (SEI) model by Jorgensen and Pranata.¹⁴ In this model, the bond strength is related to the diagonal (i.e., secondary) interactions between two adjacent hydrogen bonds, which can either be attractive (green arrows in Figure 1a) or repulsive (red arrows in Figure 1a). When two hydrogen bond donor atoms D (with a partial positive charge) are on one monomer and both hydrogen bond acceptor atoms A (with a partial negative charge) are on the other monomer, the diagonal interactions in the resulting DD–AA dimer will be attractive. On the other hand, when the donor and acceptor atoms are alternating, such as in DA–AD dimers, the resulting diagonal interactions will be repulsive. The model thus assumes that the hydrogen bond strength can be increased by maximizing the number of attractive while minimizing the number of repulsive SEIs. Indeed, there are impressive

examples of DDD–AAA and DDDD–AAAA systems with exceptionally high binding strengths.^{15–19}

Despite the model's successful predictions for hydrogen bond strengths,^{15–22} it is rather limited for further tuning the hydrogen bond strength. This is because the SEI model views hydrogen bonds as interacting point charges and does not consider any other bonding components that contribute to the binding strength.^{23–26} Hence, besides increasing the number of attractive interactions, the model does not provide chemists with any other design principles to influence hydrogen bond stability. However, by considering the origin of the predictive power of the SEI model, we can actually obtain simple tools to further tune the hydrogen bond strength.

To understand this in more detail, we take one step back and quickly recap the actual nature of hydrogen bonds, which are not only electrostatic but also partly covalent in nature.^{24–29} This covalent component originates from the donation of electron density from the lone pair orbital on the acceptor atom A into the antibonding σ^* orbital on the hydrogen bond donor group D (Figure 1b). In addition, there are a number of

Received: August 27, 2020
Revised: October 1, 2020
Published: October 15, 2020



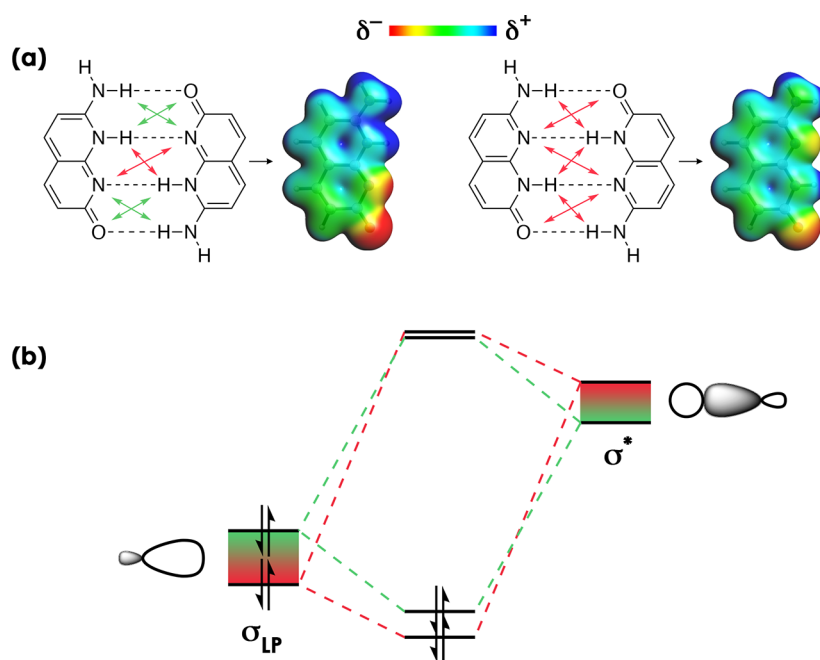


Figure 1. (a) In systems with attractive SEIs (green arrows), there is a larger monomeric charge accumulation than in systems with repulsive SEIs (red arrows). This larger accumulation of charge enhances both the electrostatic interaction and orbital interaction in the resulting dimer.²⁵ (b) Larger accumulation of negative charge around the hydrogen bond acceptor group destabilizes the σ -lone pair orbital, while a larger accumulation of positive charge around the hydrogen bond-donating group stabilizes the σ^* orbital. This results in a decrease in the highest occupied molecular orbital (HOMO)–lowest unoccupied molecular orbital (LUMO) gap and therefore a better orbital interaction when the charge accumulation is more pronounced. The green and red colors refer to a stronger and weaker orbital interaction, respectively.

other bonding components that contribute to the hydrogen bond strength, including Pauli repulsive interactions,³⁰ π -resonance assistance^{31–34} dispersion interactions,³⁵ and cooperative effects.^{36–39} An overview of the different components that contribute to hydrogen bond formation is given in ref 24.

The reason that the SEI model is predictive is that in systems with attractive SEIs there is a larger monomeric charge accumulation around the frontier atoms (Figure 1a).²⁵ This charge accumulation makes the acceptor atoms A more negative and donor atoms D more positive, which enhances (1) the electrostatic interaction and (2) the orbital interaction. The electrostatic interaction is mainly enhanced because the primary interactions, i.e., the hydrogen bonds, are formed between atoms with larger partial charges. The orbital interaction is strengthened because a positive charge accumulation around the donor atoms stabilizes the LUMO, while a negative charge accumulation around the acceptor atoms destabilizes the HOMO (Figure 1b). Hence, the accumulation of charge results in a smaller HOMO–LUMO gap and therefore a better orbital interaction.^{24,25}

It follows from these insights that the hydrogen bond strength can be tuned by modifying the charge accumulation in the monomers. This can be accomplished not only by increasing the number of attractive secondary interactions²⁵ but also by other molecular modifications such as the introduction of substituents on remote positions.^{40–44} This has for example been done successfully for the Watson–Crick DNA base pair guanine–cytosine by Fonseca Guerra and co-workers⁴⁰ and for enamione derivatives by Gilli and Gilli.⁴¹ Rocha-Rinza and co-workers showed that the hydrogen bond strength is enhanced with increased acidity and basicity of the hydrogen bond donor and acceptor groups, respectively.^{45,46}

The tunability with remote substituents has also been studied by numerous groups for supramolecular building blocks.^{47–50} Sijbesma et al. studied the association behavior of several DAD–ADA systems and acylated derivatives.⁴⁷ They found that the association constant is increased approximately tenfold by acetylation of the DAD monomer 2,6-diaminopyridine, which was attributed to an increased acidity of the hydrogen bond donor groups D. Wilson et al. investigated the effect of electron-withdrawing groups (EWGs) and electron-donating groups (EDGs) on monomers with DDA and AAD motifs.⁴⁸ They illustrated that the association constant is increased by up to two orders of magnitude with remote EDGs on AAD and with remote EWGs on DDA, the latter being accompanied by an increased positive charge accumulation around the hydrogen bond donor groups.

In the current work, we aim to tune the hydrogen bond strength in a rational way by increasing the charge accumulation around the frontier atoms using EWG CN and EDG NH₂ as remote substituents. We start by substituting a simple pyridine...H₂O model system as a proof of principle. Subsequently, we go to the tautomeric quadruple DDAA–AADD and DADA–ADAD systems that were studied in ref 25 and finally to the triple hydrogen-bonded DDA–AAD and DAD–ADA dimers. Our results show that these simple tuning tools are successful for the single and triple hydrogen-bonded systems but more difficult for quadruple hydrogen-bonded systems because of the cancellation of counteracting substituent effects. We therefore conclude that these design tools are mainly suitable for monomers with an unequal number of hydrogen bond donor and acceptor groups.

2. COMPUTATIONAL METHODS

2.1. Computational Settings. All calculations were performed using the density functional theory (DFT)-based program Amsterdam Density Functional (ADF) 2017.208.^{51–53} We used the dispersion-corrected BLYP-D3(BJ) functional in combination with a TZ2P basis set for geometry optimizations and energies,^{54–57} which accurately reproduces the structural and energetic properties of hydrogen-bonded systems.^{58–60} The hydrogen bond strength was computed by subtracting the energy of the fully optimized monomers from the energy of the dimer that is formed by these monomers,

$$\Delta E = E_{\text{dimerAB}} - E_{\text{monomerA}} - E_{\text{monomerB}}$$

All optimizations were done using C_1 (i.e., without) symmetry constraints. The molecular figures were illustrated using CYLview.⁶¹ Full computational details are available in Supporting Information Methods 1.

2.2. Voronoi Deformation Density (VDD) Charges.

The atomic charge distribution is analyzed using the Voronoi deformation density (VDD) method.⁶² The VDD method partitions the space into the so-called Voronoi cells, which are nonoverlapping regions of space that are closer to nucleus A than to any other nucleus. The charge distribution is determined by taking a fictitious promolecule as a reference point, in which the electron density is simply the superposition of the atomic densities. The change in density in the Voronoi cell when going from this promolecule to the final molecular density of the interacting system is associated with the VDD atomic charge Q_A . Thus, the VDD atomic charge Q_A^{VDD} of atom A is given by

$$Q_A^{\text{VDD}} = - \int_{\text{Voronoi cell of A}} [\rho(r) - \rho_{\text{promolecule}}(\mathbf{r})] \text{d}\mathbf{r}$$

Instead of computing the amount of charge contained in the atomic volume, we thus compute the flow of charge from one atom to the other upon formation of the molecule. The physical interpretation is therefore straightforward. A positive atomic charge Q_A corresponds to the loss of electrons, whereas a negative atomic charge Q_A is associated with the gain of electrons in the Voronoi cell of atom A.

3. RESULTS AND DISCUSSION

3.1. Pyridine \cdots H₂O Systems. We start with a simple model system, namely, the interaction between pyridine and H₂O. Pyridine was substituted with NH₂ and CN on either the meta or para position from N. The ortho position was not included to prevent the formation of additional hydrogen bonds between the substituents and the water molecule. Since NH₂ is electron-donating in nature,⁶³ it is expected to strengthen the hydrogen bond by making the nitrogen atom more negative. On the other hand, the electron-withdrawing CN group⁶³ is expected to make the nitrogen atom less negative, resulting in weakening of the hydrogen bond strength.

As can be seen in Figure 2a, the substituent effects are indeed exactly as anticipated. The hydrogen bond strength for the unsubstituted pyridine \cdots H₂O system is -7.9 kcal mol⁻¹. The substitution with EWG CN results in weakening the strength by 1.0 and 1.2 kcal mol⁻¹ for the para and meta positions, respectively, which is accompanied by a slight increase of the hydrogen bond length and a decrease of the

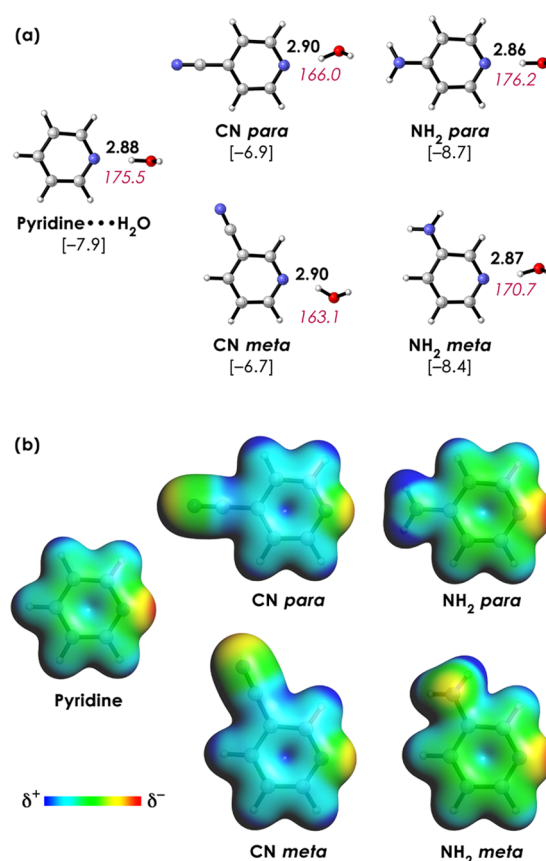


Figure 2. (a) Hydrogen bond energies in brackets (in kcal mol⁻¹), N–O bond lengths in bold (in Å), and N–H–O bond angles in red italic (in degrees) for the pyridine \cdots H₂O systems. (b) Electrostatic potential surfaces (at 0.01 Bohr⁻³) from -0.1 (red) to 0.1 (blue) Hartree e⁻¹ for the prepared monomers, i.e., the monomers with the same geometry as in the interacting dimer. All data were obtained at the BLYP-D3(BJ)/TZ2P level of theory.

hydrogen bond angles in comparison with the unsubstituted pyridine \cdots H₂O system. Interestingly, resonance structures (Supporting Information Figure 1) predict the accumulation of electronic density of the π -system due to the substituent to be most pronounced on the ortho and para position (see also ref 64). However, we find that the substituent effect with CN is even slightly more pronounced on the meta position, which shows that these simple resonance structures are not always successful in predicting substituent effects and inductive effects should also be taken into account. Substituting with EDG NH₂ results in the strengthening of the hydrogen bond by 0.8 and 0.5 kcal mol⁻¹ for the para and meta positions, respectively, which is accompanied by a slight decrease of the hydrogen bond lengths. The hydrogen bond angles N \cdots H–O tend to be closer to 180° when substituted with NH₂ than with CN.

Next, we further rationalize the changes in hydrogen bond strength by analyzing the electrostatic potential surfaces (EPSs) of the prepared monomers. As can be seen in Figure 2b, the negative charge accumulation around the hydrogen bond acceptor atom N becomes less pronounced (i.e., less red) when substituted with CN in comparison to the unsubstituted system. This is perfectly in line with the fact that CN is electron-withdrawing in nature. On the other hand, the charge accumulation around N becomes more pronounced with EDG NH₂. This enhancement of negative charge is larger when NH₂

is substituted at the para position, in agreement with its larger increase in hydrogen bond strength.

We subsequently analyzed the σ -lone pair energies of the hydrogen bond acceptor atom N (Supporting Information Figure 2). Recall from Figure 1b that enhanced accumulation of charge will result in destabilization, while a diminished accumulation of charge results in stabilization of the orbital energy. For EWG CN, the diminished accumulation of charge does indeed result in stabilization of the HOMO by 0.7 eV, for both the para and meta positions. As the LUMO energy is the same for all systems (because the hydrogen bond is always formed with H₂O), the HOMO–LUMO gap is larger for systems with CN as the remote substituent. This results in weakening of the orbital interaction and hence weakening of the hydrogen bond energy. The σ -lone pair for pyridine with NH₂ is destabilized by 0.3 and 0.2 eV at the para and meta positions, respectively. This is in line with the fact that NH₂ at para has a more pronounced strengthening effect on the hydrogen bond energy than NH₂ at the meta position.

Overall, these results demonstrate that the hydrogen bond is indeed tunable in a predictable way by altering the charge accumulation of the frontier atom with remote substituents. We will now continue to use this principle on larger molecular systems, namely, DDAA–AADD and DADA–ADAD dimers.

3.2. Quadruple Hydrogen-Bonded Tautomers. Now that we understand the substituent effects of NH₂ and CN for the simple pyridine...H₂O model system, we go to the quadruple hydrogen-bonded systems DDAA–AADD and DADA–ADAD (Figure 3a). The DDAA and DADA monomers can be substituted on four different positions, namely, at positions 1–4 (see Figure 3b for atomic numbering and Figures 4 and 5 for molecular structures). However, only CN has been substituted at all four positions because NH₂ forms intramolecular hydrogen bonds with the outer amine and carbonyl groups of the monomers, which has pronounced effects on the hydrogen bond strength.⁶ Since we are purely interested in the remote substituent effects, we have therefore substituted NH₂ on positions 2 and 3 only. The names of the molecular systems include the type and position of the substituent in parentheses. For example, DDAA–AADD with CN substituted on position 1 is named DDAA(CN,1)–AADD(CN,1).

In this manuscript, we only consider the homodimers, as these already reveal the substituent effects that are the subject of our study. However, we have also computed the dimers in which only one of the two monomers has been substituted (Supporting Information Figure 3). For these heterodimers with NH₂ as the remote substituent, we find that the energetic changes are approximately halved with respect to their corresponding homodimers, which is in line with the fact that we go from two substituted monomers to only one. When substituted with CN, we find for all dimers except for DADA(CN,4) that going from two to one substituted monomer results in a small lowering of the hydrogen bond energy, which is likely caused by long-range electrostatic interactions (vide infra).

Before going to the substituted systems, we consider the properties of the unsubstituted DDAA and DADA monomers and dimers. It is known from previous work²⁵ that DDAA–AADD has stronger interactions than DADA–ADAD because of its more pronounced monomeric charge accumulation, which enhances both the electrostatic interaction and orbital interactions in the dimer. This charge accumulation is nicely

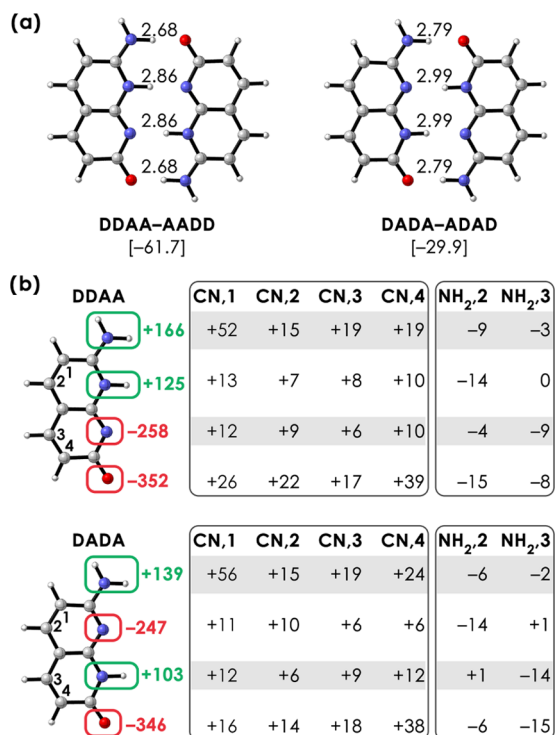


Figure 3. (a) Hydrogen bond strength ΔE (in kcal mol⁻¹) and O...N or N...N bond lengths (in Å) of the unsubstituted DDAA (left) and DADA (right) dimers. (b) Voronoi deformation density (VDD) charges (in me⁻) of the hydrogen bond donor (green rectangles) and acceptor (red rectangles) groups of the prepared unsubstituted monomers, and the change in VDD charge for the same hydrogen bond donor and acceptor groups when substituted with CN or NH₂. For example, the VDD charge of the NH₂ group in DDAA becomes 52 me⁻ more positive when going from DDAA to DDAA(CN,1). All data were obtained at the BLYP-D3(BJ)/TZ2P level of theory.

revealed by electrostatic potential surfaces (EPSs, Figure 1a). However, the disadvantage of using these EPSs in combination with remote substituents is that the changes in charge accumulation caused by the substituents are relatively small in comparison with the intrinsic charge accumulation in the unsubstituted systems. Hence, a more suitable way to probe the substituent effects is by analyzing the Voronoi deformation density (VDD) charges, which are given in Figure 3b. The VDD charges show that the hydrogen bond donor groups have a larger positive charge, while the hydrogen bond acceptor groups have a larger negative charge in DDAA than in DADA, which is perfectly in line with the EPSs in Figure 1a. This larger accumulation of negative charge destabilizes the lone pair orbitals, while the larger accumulation of positive charge stabilizes the σ -LUMO orbitals (Figure 6a), resulting in a smaller HOMO–LUMO gap and hence a stronger orbital interaction.

We now address the question of how the hydrogen bond strength, VDD charges, and orbital energies are affected by the remote substituents. We start by considering the quadruple hydrogen-bonded dimers that are substituted with the electron-withdrawing CN group (Figure 4). Overall, we see that all hydrogen bond donor groups become more positive, while all hydrogen bond acceptor atoms become less negative with CN as the remote substituent (Figure 3b). This is accompanied by stabilization of all molecular orbitals (Figure 6b). Initially, we expected that these substituent effects would

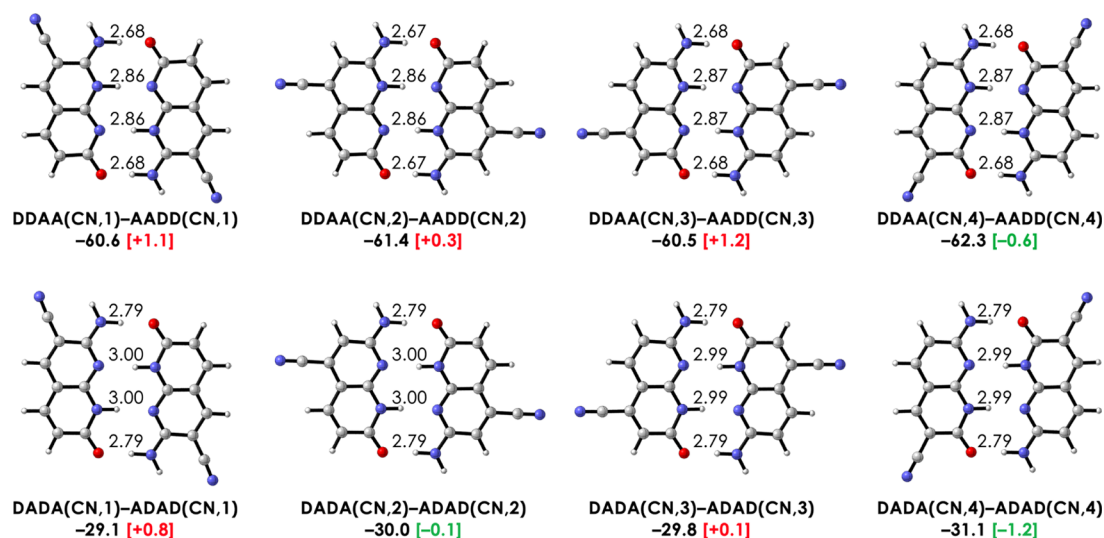


Figure 4. Hydrogen bond strength ΔE (in kcal mol⁻¹) and O...N or N...N bond lengths (in Å) for the DDAA (up) and DADA (down) homodimers with CN substitution at position 1, 2, 3, or 4. The value in brackets gives the difference relative to the unsubstituted dimer. All data were obtained at the BLYP-D3(BJ)/TZ2P level of theory.

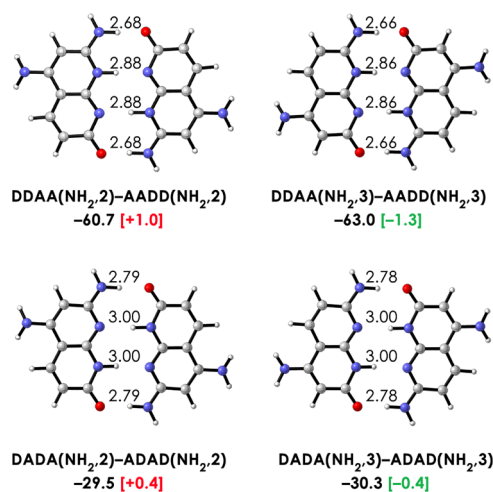


Figure 5. Hydrogen bond strength ΔE (in kcal mol⁻¹) and O...N or N...N bond lengths (in Å) for the DDAA (up) and DADA (down) homodimers with NH₂ substitution at position 2 or 3. The value in brackets gives the difference relative to the unsubstituted dimer. All data were obtained at the BLYP-D3(BJ)/TZ2P level of theory.

be most pronounced for the nearest frontier atoms, which would make the tunability of the DDAA–AADD dimers fairly straightforward. However, the substituent effects are actually delocalized over the whole molecular system, making it very difficult to predict how the hydrogen bond interactions are affected by the substituent.

To understand this in more detail, we consider the DDAA system with CN at position 1. If the nearest frontier atoms would be most affected by the substituent, CN at position 1 would cause strengthening of the hydrogen bond because of enhanced positive charge accumulation around the hydrogen bond donor groups. However, as can be seen in Figure 4, the DDAA(CN,1)–AADD(CN,1) dimer is actually 1.1 kcal mol⁻¹ less stable than the unsubstituted DDAA–AADD dimer. At first sight, the substituent CN does indeed have the most pronounced effect on the nearby NH₂ group, which becomes 52 me⁻ more positive in comparison with the unsubstituted

group, whereas NH, N, and O become more positive by 13, 12, and 26 me⁻, respectively. However, the lone pair orbitals of the hydrogen bond acceptor groups are actually more stabilized than the virtual orbitals (Figure 6b), even though the occupied orbitals are farther away from the substituent than the virtual orbitals. As a result, the substituent CN actually leads to an increase instead of a decrease of the HOMO–LUMO gap, which explains why the total hydrogen bond strength is weakened by CN at position 1.

For substitution with CN at position 4, the hydrogen bond acceptor atoms N and O are the nearest to the substituent. We therefore expected that the substituent effect would be most pronounced on N and O, resulting in diminished charge accumulation around N and O and hence weakening of the hydrogen bond. However, the hydrogen bond energy of DDAA(CN,4)–AADD(CN,4) is in fact more stable with respect to the unsubstituted dimer by -0.6 kcal mol⁻¹. Looking at the VDD charges in Figure 3b, we see that the hydrogen bond acceptor atoms become less negative by 49 me⁻ in total, whereas the hydrogen bond donor groups become more positive by 29 me⁻ in total. Hence, the substituent effects are delocalized over the whole molecular system but more pronounced for the acceptor atoms. Consulting the orbital energies in Figure 6b, we find that the lone pair orbitals are stabilized to a larger extent than the σ^* orbital, resulting in a net increase of the HOMO–LUMO gap. Neither the VDD charges nor the orbital energies thus explain the resulting stabilization of the hydrogen bond energy. However, there is a third factor that we did not consider so far, which is the long-range electrostatic interaction between the interacting monomers, including the interactions between the substituent and the other monomer.

To further understand this effect, we divided the monomers into three regions and computed the sum of atomic VDD charges for each region (Figure 7). For the unsubstituted DDAA monomer, the upper region (blue rectangle), which includes both hydrogen bond donor groups, has a partial positive charge of +392 me⁻. On the other hand, the lower region (red rectangle) includes both hydrogen bond acceptor groups and has a partial negative charge of -459 me⁻. The

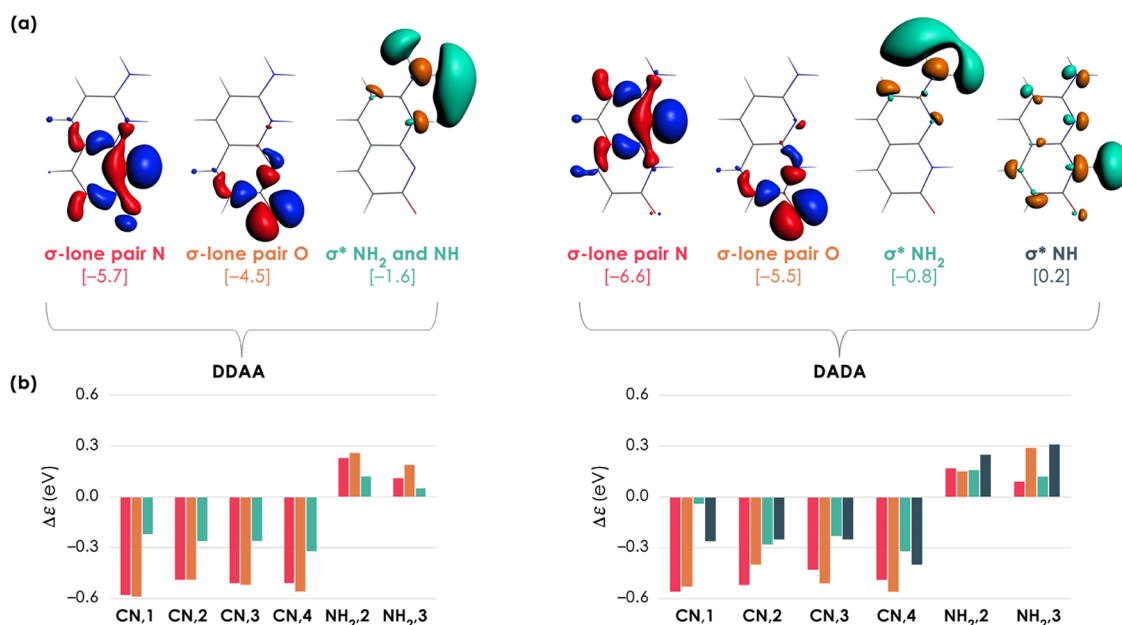


Figure 6. (a) Isosurfaces (at 0.04 Bohr^{-3/2}) and energies (in eV) of the orbitals of the prepared monomers that participate in orbital interactions. (b) Change in orbital energy (in eV) when DDAA (left) or DADA (right) is substituted with CN or NH₂. The colors correspond to the text color in Figure 6a. All data were obtained at the BLYP-D3(BJ)/TZ2P level of theory.

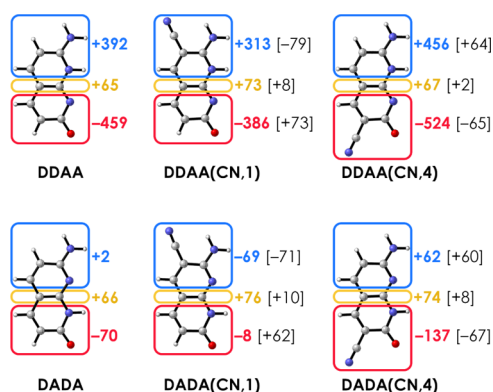


Figure 7. Voronoi deformation density charges (in me⁻) for the prepared DDAA (up) and DADA (down) monomers without substituents (left) and with substituents (middle and right). Data was obtained at the BLYP-D3(BJ)/TZ2P level of theory.

atoms that connect these two regions (yellow rectangle) have a small positive charge of +65 me⁻. Note that this charge delocalization is perfectly in line with the electrostatic potential surface in Figure 1a. So, how is this charge delocalization affected by the substituents? We start with DDAA(CN,4), whose red region now also contains the electron-withdrawing CN substituent. As a result, this region becomes 65 me⁻ more negative in comparison with the unsubstituted system. This charge is mainly coming from the blue region, which becomes 64 me⁻ more positive in comparison with the unsubstituted system. Hence, even though the charge accumulation around the frontier atoms is slightly unfavorable (Figure 3b) for DDAA(CN,4), the charge redistribution in the overall system is actually favorable for its dimerization energy. After all, the blue region is now more positive, while the red region is now more negative, resulting in stronger electrostatic interactions and hence a stronger binding strength.

Going to the DDAA(CN,1) monomer, the blue region becomes less positive by -79 me⁻, while the red region

becomes less negative by +73 me⁻ in comparison with the unsubstituted system. In this case, the charge redistribution is thus unfavorable for the dimerization energy because the regions have a smaller partial charge, resulting in weaker electrostatic interactions. This is again perfectly in line with the observed weakening of the binding energy in the DDAA-(CN,1) dimer. These results show that the substituent does not only affect the charge accumulation around the frontier atoms but instead affects the charge redistribution in the whole molecular system, which must be taken into account when tuning the binding strength of hydrogen-bonded arrays.

For the DDAA(CN,2) dimer, the hydrogen bonding is less stable by 0.3 kcal mol⁻¹ in comparison with the unsubstituted system (Figure 4). The hydrogen bond donor groups become more positive by 22 me⁻ in total, whereas the hydrogen bond acceptor atoms become less negative by 31 me⁻ in total (Figure 3b). Furthermore, the occupied orbitals are more stabilized than the virtual orbitals, resulting in a larger HOMO–LUMO gap and hence a weakened orbital energy (Figure 6b). Both the charge redistribution and orbital energies are thus in line with the observed destabilization of ΔE . However, the DDAA(CN,3) dimer is destabilized by 1.2 kcal mol⁻¹, which is considerably more pronounced than for the DDAA(CN,2) dimer. This difference in ΔE cannot be explained by the change in charge accumulation around the frontier atoms, which is almost the same for the hydrogen bond donor groups (+27 me⁻) as for the hydrogen bond acceptor atoms (+23 me⁻), and neither with the HOMO–LUMO gap, which is increased by approximately the same amount as for the DDAA(CN,2) dimer. Furthermore, the long-range electrostatic interactions do also not explain the relatively large destabilization of DDAA(CN,3)–AADD-(CN,3) because, similarly to DDAA(CN,4) (Figure 7), CN at position 3 should lead to more pronounced charge accumulation. Other factors are at play, which underlines the complex nature of hydrogen bonds in multiple hydrogen-bonded arrays.

Next, we go to the DADA–ADAD systems with CN as a substituent. As these molecules have an alternating pattern of hydrogen bond donor and acceptor groups, we expected that these systems are more difficult to tune because the substituent will have a counteracting effect on two neighboring atoms. However, as can be seen in Figure 4, the hydrogen bond strength is actually changed by comparable values as for the DDAA systems. The substitution with CN at position 1 leads to a weakening of $0.8 \text{ kcal mol}^{-1}$, whereas CN at position 4 leads to strengthening of the hydrogen bond energy by $1.2 \text{ kcal mol}^{-1}$ with respect to the unsubstituted DADA dimer. The hydrogen bond strength with CN at positions 2 and 3 remains approximately unchanged. By consulting the VDD charges (Figure 3b) and orbital energies (Figure 6b), we find the same results as for the DDAA systems. That is, the substituent effects are again delocalized over the whole molecular system, which is evident from the loss of electronic density for all frontier atoms and stabilization of all molecular orbitals. This stabilization is more pronounced for the occupied lone pair orbitals than for the virtual σ^* orbitals, resulting in increased HOMO–LUMO gaps for all four systems. These findings do explain the weakening of DADA(CN,1)–ADAD(CN,1) but not why CN at position 4 leads to a more stable hydrogen bond energy. However, by consulting the monomeric charge redistribution in Figure 7, we see that the blue region in DADA(CN,4) becomes more positive by 60 me^- , while the red region becomes more negative by 67 me^- in comparison with DADA. Hence, the overall charge redistribution is actually favorable for the dimerization energy due to the long-range electrostatic interactions, which is the same as already encountered for the DDAA(CN,4) dimer.

We then go to the electron-donating NH_2 substituent, which has been substituted at positions 2 and 3 of the DDAA and DADA monomers (Figure 5). In general, the hydrogen bond donor groups become less positive while the hydrogen bond acceptor atoms become more negative in comparison with the unsubstituted system (Figure 3b), which is accompanied by destabilization of all molecular orbitals (Figure 6b). However, these changes are smaller than obtained with CN as the remote substituent, which is in line with our findings for pyridine... H_2O (Figure 2). For NH_2 at position 2, we see that the charge redistribution in DDAA is again delocalized over the whole molecular system and that there is no prominent difference between the changes in VDD charge for the hydrogen bond donor (-23 me^-) and acceptor groups (-19 me^-). There is a more noticeable difference between the changes in orbital energies, which undergo a more pronounced destabilization for the σ lone pairs than for the σ^* orbital on NH_2 and NH . However, despite the resulting net decrease in the HOMO–LUMO gap, the DDAA($\text{NH}_2,2$) dimer is actually $1.0 \text{ kcal mol}^{-1}$ less stable than the unsubstituted system. A possible explanation might again be the long-range electrostatic interactions between the interacting monomers, but as one of the hydrogens of the NH_2 substituent is now partly overlapping with the yellow region, the analysis as done in Figure 7 is less straightforward for this specific system.

For DDAA($\text{NH}_2,3$)–AADD($\text{NH}_2,3$), the hydrogen bond energy is strengthened by $1.3 \text{ kcal mol}^{-1}$. This is not only in line with a greater increase of negative charge around the hydrogen bond acceptor atoms (-17 me^-) in comparison with the hydrogen bond donor groups (-3 me^-) but also with a decrease in the HOMO–LUMO gap. Finally, NH_2 at positions 2 and 3 in the DADA systems results in the same but less

pronounced trend than for the DDAA systems. That is, the hydrogen bond strength is weakened by $0.4 \text{ kcal mol}^{-1}$ on position 2, and strengthened by $0.4 \text{ kcal mol}^{-1}$ at position 3. However, contrary to the trends found so far, the virtual orbitals are affected by approximately the same amount as the occupied orbitals, resulting in an almost unchanged HOMO–LUMO gap.

Summarizing our findings up to here, we see that the hydrogen bond strength of the DDAA and DADA dimers is more difficult to tune than anticipated. This is mainly because the redistribution of charge after substitution is delocalized over the whole molecular system. Since each monomer has the same number of hydrogen bond donor and acceptor atoms, the substituent effects counteract and thus cancel each other, resulting in very small and unpredictable effects. Hence, tuning the hydrogen bond strength should be easier for systems with an unequal number of donor and acceptor atoms. We have investigated this with two DAA–ADD and ADA–DAD systems, which will be further discussed in the next section.

3.3. Triple Hydrogen-Bonded Tautomers. We have investigated two triple hydrogen-bonded systems, namely, the DAA–ADD and ADA–DAD dimers (Figure 8). These systems were obtained by removing the upper hydrogen bond in the quadruple hydrogen-bonded systems while

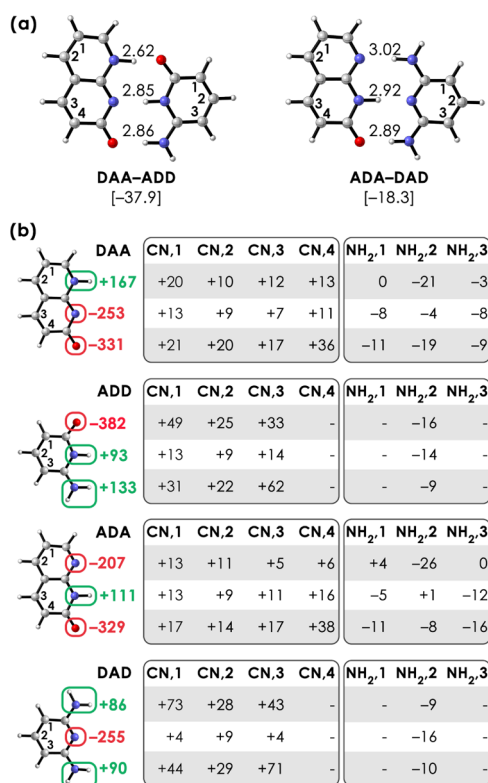


Figure 8. (a) Hydrogen bond strengths ΔE (in kcal mol^{-1}) and O...N or N...N bond lengths (in Å) of the unsubstituted DAA–ADD (left) and ADA–DAD (right) dimers. (b) Voronoi deformation density (VDD) charges (in me^-) of the hydrogen bond donor (green rectangles) and acceptor (red rectangles) groups of the prepared unsubstituted monomers, and the change in VDD charge for the same hydrogen bond donor and acceptor groups when substituted with CN or NH_2 . For example, the VDD charge of the NH group in DAA becomes 20 me^- more positive when going from DAA to DAA(CN,1). All data were obtained at the BLYP-D3(BJ)/TZ2P level of theory.

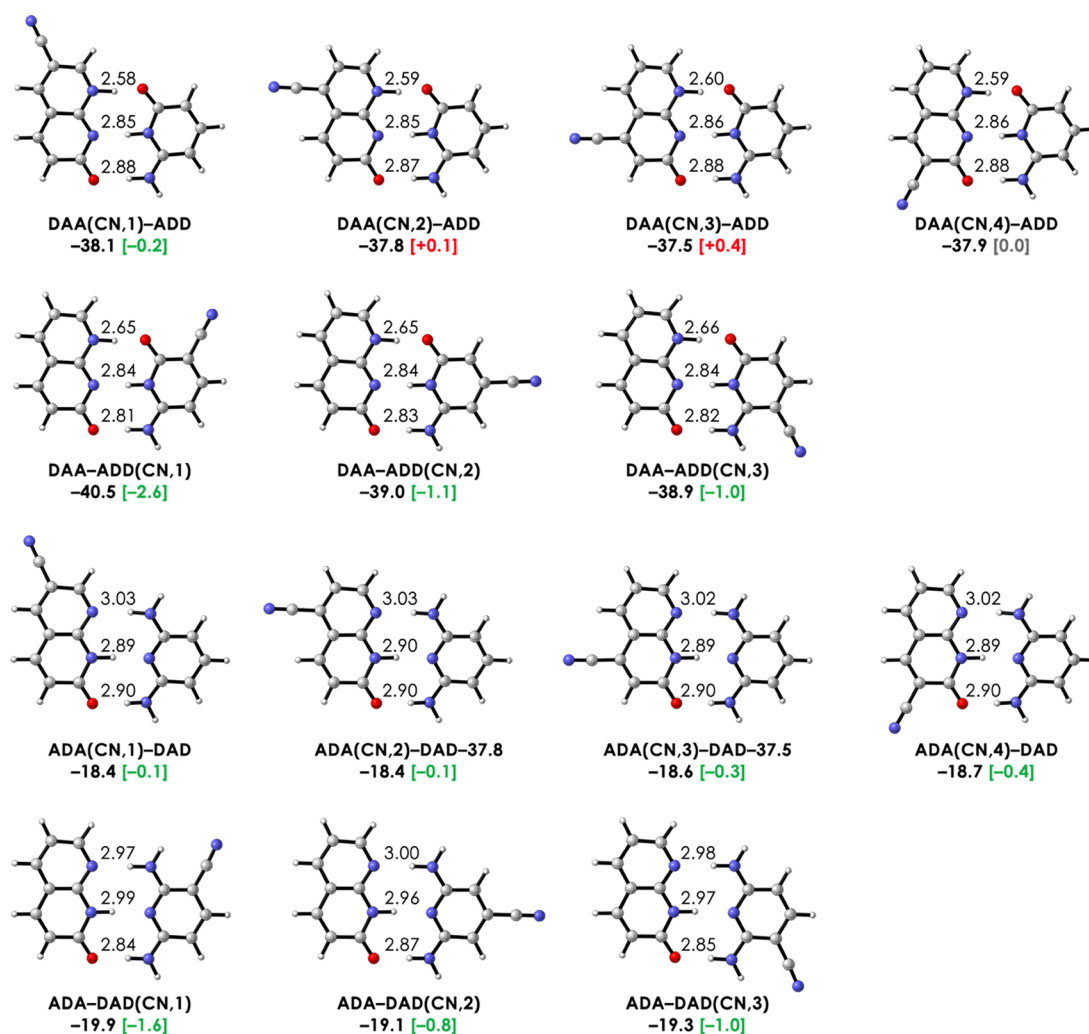


Figure 9. Hydrogen bond strengths ΔE (in kcal mol⁻¹) and O...N or N...N bond lengths (in Å) for the DAA-ADD (upper two rows) and ADA-DAD (lower two rows) dimers with CN substitution at position 1, 2, 3, or 4. The value in brackets gives the difference relative to the unsubstituted dimer. All data were obtained at the BLYP-D3(BJ)/TZ2P level of theory.

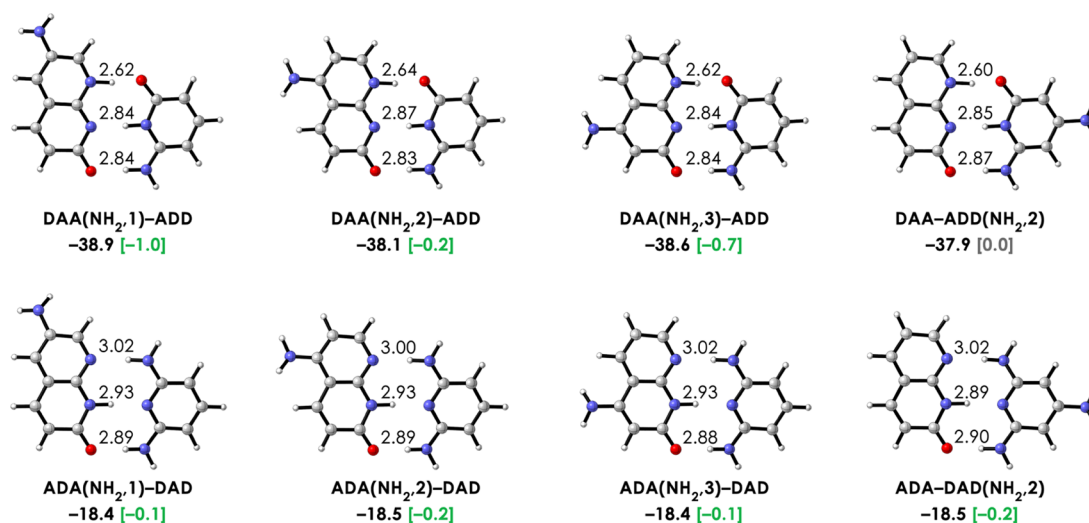


Figure 10. Hydrogen bond strengths ΔE (in kcal mol⁻¹) and O...N or N...N bond lengths (in Å) for the DAA-ADD (up) and ADA-DAD (down) dimers with NH₂ substitution at position 1, 2, or 3. The value in brackets gives the difference relative to the unsubstituted dimer. All data were obtained at the BLYP-D3(BJ)/TZ2P level of theory.

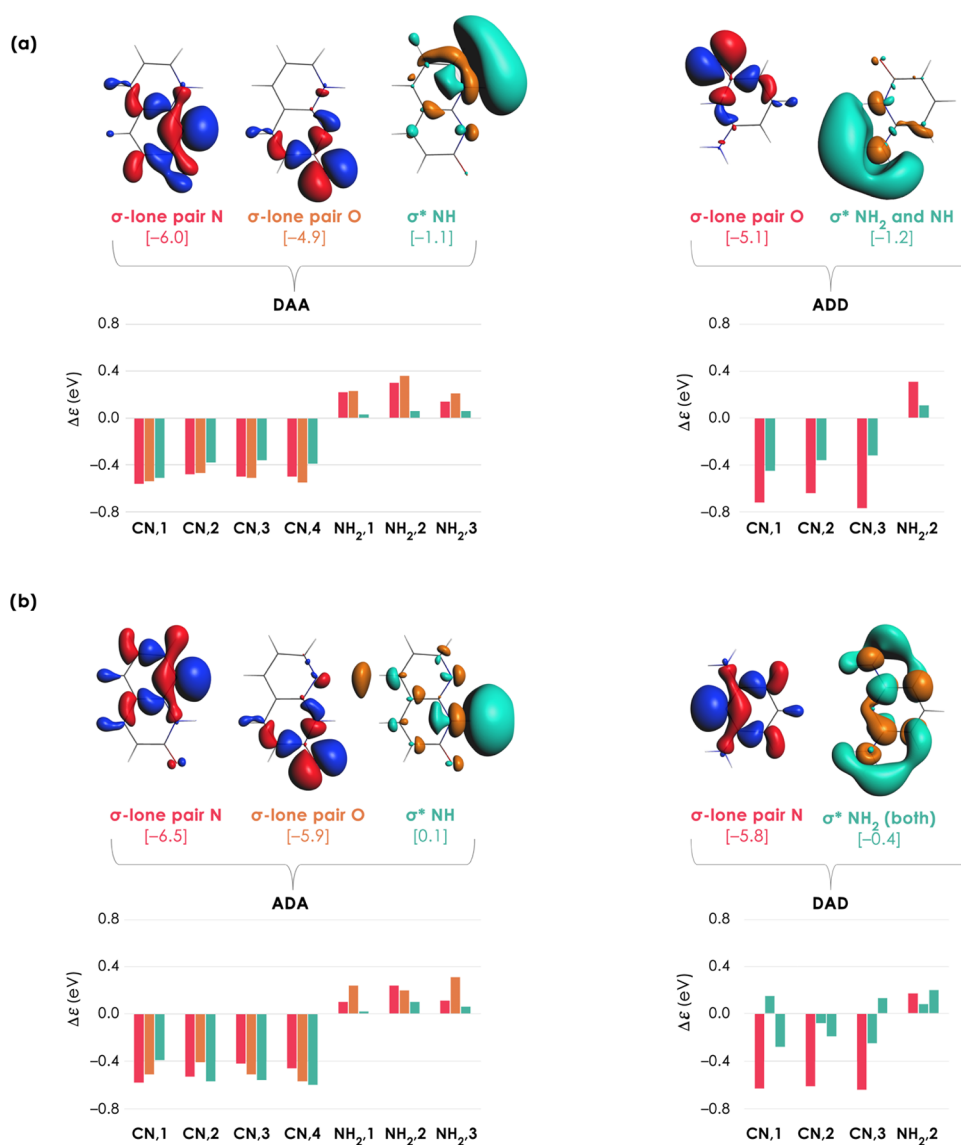


Figure 11. (a) Isosurfaces (at $0.03 \text{ Bohr}^{-3/2}$) and energies (in eV) of the orbitals of the prepared DAA and ADD monomers that participate in orbital interactions and the change in orbital energy (in eV) when DAA (left) or ADD (right) is substituted with CN or NH_2 . The colors correspond to the text color in (a). (b) Isosurfaces (at $0.03 \text{ Bohr}^{-3/2}$) and energies (in eV) of the orbitals of the prepared ADA and DAD monomers that participate in orbital interactions, and the change in orbital energy (in eV) when ADA (left) or DAD (right) is substituted with CN or NH_2 . The colors correspond to the text color in (b). All data were obtained at the BLYP-D3(BJ)/TZ2P level of theory.

maintaining a conjugated system. We used the same substituents as for the quadruple hydrogen-bonded systems, i.e., EWG CN and EDG NH_2 . Because of the hydrogen bond pattern, these monomers cannot dimerize with itself but form heterodimers instead. The heterodimers were formed with one substituted and one unsubstituted monomer, resulting in one substituent per dimer. We named the molecular systems in the same way as the quadruple systems. For example, a DAA–ADD dimer with CN on position 2 at DAA is called DAA(CN,2)–ADD (the atomic numbering is given in Figure 8). CN has been substituted at all possible positions, i.e., positions 1–4 in DAA and ADA and positions 1–3 in ADD and DAD, whereas NH_2 has only been substituted at positions 1–3 in DAA and ADA and position 2 in ADD and DAD to prevent the formation of intramolecular hydrogen bonds. The systems substituted with CN are shown in Figure 9, and the systems substituted with NH_2 are shown in Figure 10.

We start with the systems substituted with CN. It can be seen in Figure 8b that substitution with CN makes all hydrogen bond donor groups more positive while making all hydrogen bond acceptor groups less negative. This is accompanied by stabilization of all molecular orbitals (Figure 11), except for one of the virtual orbitals in DAD(CN,1) and DAD(CN,3). This means that the substituent effects of CN are favorable for the hydrogen bond donor groups (more positive and lower σ^* virtual orbital) and unfavorable for the hydrogen bond acceptor groups (less negative and lower σ lone pair orbital). As the dimers have an unequal number of donor and acceptor atoms, it is therefore expected that CN on DAA or ADA results in weakening, whereas CN on ADD or DAD results in strengthening of the hydrogen bonds.

As can be seen in Figure 9, the dimers with CN on ADD or DAD are considerably more affected than the dimers with CN on DAA or ADA. For the DAA(CN)–ADD and ADA(CN)–DAD dimers, the change in hydrogen bond energy varies

between $+0.4 \text{ kcal mol}^{-1}$ for DAA(CN,3)–ADD and $-0.4 \text{ kcal mol}^{-1}$ for ADA(CN,4)–DAD only, which is small in comparison with the changes observed for pyridine \cdots H₂O and the quadruple hydrogen-bonded systems. It is surprising that the hydrogen bond strength is not much destabilized when CN is substituted on DAA or ADA, even though these monomers have two hydrogen bond acceptor groups. A possible explanation might again be the long-range electrostatic interactions between the partially negatively charged substituents and positively charged hydrogen bond-donating groups on the opposing monomer.

Interestingly, the dimers with CN on ADD or DAD are all stabilized by a substantial amount in comparison with the unsubstituted system. As the ADD and DAD monomers have two hydrogen bond donor groups, these changes in binding energy are in line with the expectations. For the DAA–ADD(CN) dimer, the hydrogen bonding is stabilized by 2.6, 1.1, and 1.0 kcal mol^{-1} for positions 1–3, respectively. This shows that the position of the substituent plays an important role in the observed changes in the binding strength. As CN at position 1 is the farthest from the hydrogen bond donor groups but causes the largest stabilization of ΔE , these results underline the fact that the substituent effects are not limited to the nearest frontier atoms but are instead delocalized over the whole molecular system. At this point, it is important to emphasize that relatively small differences in the binding energy are associated with large changes in the binding constant K ; a Gibbs free energy stabilization of $2.7 \text{ kcal mol}^{-1}$ corresponds to a 100-fold increase in the binding constant K .³ Hence, these substituent effects can have profound effects on self-assembling polymer systems.

For the ADA–DAD(CN) dimer, the hydrogen bond strengths are stabilized by 1.6, 0.8, and 1.0 kcal mol^{-1} for positions 1–3, respectively. This shows again that the position of the substituent has a large effect on the observed changes in binding strength. Comparing positions 1 and 3, we see that the changes in VDD charge and orbital energies are actually very similar, but still the stabilization of ADA–DAD(CN,1) is 0.6 kcal mol^{-1} more pronounced than for the ADA–DAD(CN,3) dimer. A reason for this might be the long-range electrostatic interaction between the substituent with a partial negative charge and the frontier atoms of the other monomer. As the nitrogen atom N on ADA has a smaller partial negative charge than O (-207 and -329 me^- for N and O respectively, see Figure 8), its destabilizing long-range interactions with CN might be less pronounced, resulting in larger net stabilization of the hydrogen bond strength.

Finally, we go to the electron-donating substituent NH₂ (Figure 10). As can be seen in Figure 8b, all hydrogen bond acceptor atoms become more negative, while all hydrogen bond donor groups become less positive, except for NH in DAA(NH₂,1), N in ADA(NH₂,1), NH in ADA(NH₂,2), and N in ADA(NH₂,3), which gain 0, 4, 1, and 0 me^- , respectively. This redistribution of charge is accompanied by destabilization of all occupied and virtual molecular orbitals (Figure 11), and this destabilization is generally more pronounced for the σ lone pair than for the σ^* virtual orbitals. For the DAA(NH₂)–ADD dimer, hydrogen bonding becomes stronger by 1.0, 0.2, and 0.7 kcal mol^{-1} for positions 1–3, respectively. As the DAA monomer has two acceptor groups, this result is in line with the expectations. Here, we see again that the substituent effect is strongly dependent on the position of the substituent.

For the other three types of dimers, namely, DAA–ADD(NH₂), ADA(NH₂)–DAD, and ADA–DAD(NH₂), the changes in hydrogen bond strength vary between 0.0 and $-0.2 \text{ kcal mol}^{-1}$. Hence, the NH₂ substituent effects are considerably smaller than the effects obtained with CN. We saw already for the pyridine \cdots H₂O that NH₂ has a less pronounced effect on the hydrogen bond strength than CN. Furthermore, by comparing the changes in VDD charges (Figure 8) and orbital energies (Figure 11) between CN and NH₂, we see that the changes obtained with NH₂ are considerably smaller than obtained with CN, which explains why the resulting changes in hydrogen bond strengths are smaller as well. We therefore conclude that hydrogen bonding is easier to tune with CN than with NH₂ as the remote substituent.

4. CONCLUSIONS

We have used remote substituents on a number of hydrogen-bonded systems to tune the hydrogen bond strength by altering the charge accumulation around the frontier atoms. Our density functional theory-based study on pyridine \cdots H₂O with NH₂ and CN substituted on the meta and para positions of pyridine shows that the electron-withdrawing CN substituent decreases the negative charge accumulation around the frontier atom N, resulting in weakening of the hydrogen bond, whereas the electron-donating NH₂ group increases the charge accumulation around N, resulting in strengthening of the hydrogen bond. These results demonstrate that simple hydrogen-bonded systems are indeed tunable in a rational way.

We subsequently applied these principles on larger hydrogen-bonded systems, namely, on quadruple DDAA–AADD and DADA–ADAD tautomers and on triple DAA–ADD and ADA–DAD dimers, using CN as an electron-withdrawing and NH₂ as an electron-donating substituent. We find that the substituent effects are not limited to the nearest frontier atoms but are instead delocalized over the whole molecular system. In general, we see that the remote substituent CN makes all hydrogen bond donor groups more positive and all hydrogen bond acceptor groups less negative, which is accompanied by stabilization of all molecular orbitals. For NH₂, we find the opposite effect. That is, the hydrogen bond donor groups become less positive, whereas the hydrogen bond acceptor atoms become more negative, which is accompanied by destabilization of all molecular orbitals.

For the quadruple hydrogen-bonded systems, the changes in hydrogen bond strengths are small, namely, between -1.3 and $1.2 \text{ kcal mol}^{-1}$, and furthermore unpredictable. This is because the monomers have the same number of donor and acceptor groups, resulting in cancellation of the counteracting substituent effects. Furthermore, we found that the substituents do not only alter the charge accumulation around the frontier atoms but instead affect the charge redistribution in the whole molecular system. Hence, the change in hydrogen bond strength is also affected by resulting changes in long-range electrostatic interactions.

For the triple hydrogen-bonded systems, the tuning is more effective with CN than with NH₂ as the substituent. Most dimers become more stable with CN as the remote substituent, but this stabilization is more pronounced with CN on an ADD or DAD monomer than on a DAA or ADA monomer, which is in line with expectations. For the DAA–ADD(CN) series, the hydrogen bond is strengthened by 2.6, 1.1, and 1.0 kcal mol^{-1} for positions 1–3, respectively, which illustrates that the

position of the substituent plays an important role in tuning the hydrogen bond strength as well. The latter seems to be caused by long-range electrostatic interactions between the substituent and the hydrogen-bonded monomer. The NH₂ substituent is less effective in tuning the hydrogen bond strength.

In summary, our results demonstrate that hydrogen bonds are tunable in a rational way using remote substituents. However, besides altering the charge accumulation of the frontier atoms, there are also other factors at play that influence the binding strength, including long-range electrostatic interactions. The principles presented in this manuscript are mainly suitable for systems with an unequal number of hydrogen bond donor and acceptor groups to prevent the cancellation of counteracting effects and can be used for tuning the strength of supramolecular building blocks.

■ ASSOCIATED CONTENT

Supporting Information

The Supporting Information is available free of charge at <https://pubs.acs.org/doi/10.1021/acs.jpca.0c07815>.

Computational details, resonance structures of benzene with CN and NH₂ as substituents, a figure showing the lone pair orbitals of pyridine with and without the remote substituent, a figure showing the quadruple hydrogen-bonded dimers in which only one of the two monomers has been substituted, and the Cartesian coordinates with absolute energies of all studied systems (PDF)

■ AUTHOR INFORMATION

Corresponding Author

Célia Fonseca Guerra – Department of Theoretical Chemistry, Amsterdam Institute of Molecular and Life Sciences (AIMMS), Amsterdam Center of Multiscale Modeling (ACMM), Vrije Universiteit Amsterdam, 1081 HV Amsterdam, The Netherlands; Leiden Institute of Chemistry, Gorlaeus Laboratories, Leiden University, 2333 CD Leiden, The Netherlands; orcid.org/0000-0002-2973-5321; Phone: +31 20 598 7627; Email: c.fonsecaaguerra@vu.nl

Authors

Stephanie C. C. van der Lubbe – Department of Theoretical Chemistry, Amsterdam Institute of Molecular and Life Sciences (AIMMS), Amsterdam Center of Multiscale Modeling (ACMM), Vrije Universiteit Amsterdam, 1081 HV Amsterdam, The Netherlands; orcid.org/0000-0002-9723-7017

Anissa Haim – Department of Theoretical Chemistry, Amsterdam Institute of Molecular and Life Sciences (AIMMS), Amsterdam Center of Multiscale Modeling (ACMM), Vrije Universiteit Amsterdam, 1081 HV Amsterdam, The Netherlands

Thor van Heesch – Department of Theoretical Chemistry, Amsterdam Institute of Molecular and Life Sciences (AIMMS), Amsterdam Center of Multiscale Modeling (ACMM), Vrije Universiteit Amsterdam, 1081 HV Amsterdam, The Netherlands

Complete contact information is available at: <https://pubs.acs.org/doi/10.1021/acs.jpca.0c07815>

Author Contributions

[§]S.C.C.L. and A.H. contributed equally to this work.

Notes

The authors declare no competing financial interest.

■ ACKNOWLEDGMENTS

We thank The Netherlands Organization for Scientific Research (NWO/CW) for financial support.

■ REFERENCES

- (1) de Greef, T. F. A.; Meijer, E. W. Supramolecular polymers. *Nature* **2008**, *453*, 171–173.
- (2) Cordier, P.; Tourmilhac, F.; Soulié-Ziakovic, C.; Leibler, L. Self-healing and thermoreversible rubber from supramolecular assembly. *Nature* **2008**, *451*, 977–980.
- (3) Steed, J. W.; Atwood, J. L. *Supramolecular Chemistry*, 2nd ed.; John Wiley & Sons Ltd: West Sussex, 2009.
- (4) Pellizzaro, M. L.; Houton, K. A.; Wilson, A. J. Sequential and phototriggered supramolecular self-sorting cascades using hydrogen-bonded motifs. *Chem. Sci.* **2013**, *4*, 1825–1829.
- (5) Yang, L.; Tan, X.; Wang, Z.; Zhang, X. Supramolecular polymers: historical development, preparation, characterization, and functions. *Chem. Rev.* **2015**, *115*, 7196–7239.
- (6) Coubrough, H. M.; van der Lubbe, S. C. C.; Hetherington, K.; Minard, A.; Pask, C.; Howard, M. J.; Fonseca Guerra, C.; Wilson, A. J. Supramolecular self-sorting networks using hydrogen-bonding motifs. *Chem. - Eur. J.* **2019**, *25*, 785–795.
- (7) Sijbesma, R. P.; Beijer, F. H.; Brunsveld, L.; Folmer, B. J. B.; Ky Hirschberg, J. H. K.; Lange, R. F. M.; Lowe, J. K. L.; Meijer, E. W. Reversible polymers formed from self-complementary monomers using quadruple hydrogen bonding. *Science* **1997**, *278*, 1601–1604.
- (8) Kushner, A. M.; Vossler, J. D.; Williams, G. A.; Guan, Z. A biomimetic modular polymer with tough and adaptive properties. *J. Am. Chem. Soc.* **2009**, *131*, 8766–8768.
- (9) Yan, X.; Li, S.; Bryant Pollock, J.; Cook, T. R.; Chen, J.; Zhang, Y.; Ji, X.; Yu, Y.; Huang, F.; Stang, P. J. Supramolecular polymers with tunable topologies via hierarchical coordination-driven self-assembly and hydrogen bonding interfaces. *Proc. Natl. Acad. Sci. U.S.A.* **2013**, *110*, 15585–15590.
- (10) Lamers, B. A. G.; Ślęczkowski, M. L.; Wouters, F.; Engels, T. A. P.; Meijer, E. W.; Palmans, A. R. A. Tuning polymer properties of non-covalent crosslinked PDMS by varying supramolecular interaction strength. *Polym. Chem.* **2020**, *11*, 2847–2854.
- (11) Zhao, G.-J.; Han, K.-L. Effects of hydrogen bonding on tuning photochemistry: concerted hydrogen-bond strengthening and weakening. *Chem. Phys. Chem.* **2008**, *9*, 1842–1946.
- (12) De Greef, T. F. A.; Smulders, M. M. J.; Wolffs, M.; Schenning, A. P. H. J.; Sijbesma, R. P.; Meijer, E. W. Supramolecular polymerization. *Chem. Rev.* **2009**, *109*, 5687–5754.
- (13) Zheng, P.; Takayama, S. J.; Mauk, A. G.; Li, H. Hydrogen bond strength modulates the mechanical strength of ferric-thiolate bonds in rubredoxin. *J. Am. Chem. Soc.* **2012**, *134*, 4124–4131.
- (14) Jorgensen, W. L.; Pranata, J. Importance of secondary interactions in triply hydrogen bonded complexes: guanine-cytosine vs uracil-2,6-diaminopyridine. *J. Am. Chem. Soc.* **1990**, *112*, 2008–2010.
- (15) Wilson, A. J. Hydrogen bonding: attractive arrays. *Nat. Chem.* **2011**, *3*, 193–194.
- (16) Blight, B. A.; Hunter, C. A.; Leigh, D. A.; McNab, H.; Thomson, P. I. T. An AAAA–DDDD quadruple hydrogen-bond array. *Nat. Chem.* **2011**, *3*, 244–248.
- (17) Blight, B. A.; Camara-Campos, A.; Djurdjevic, S.; Kaller, M.; Leigh, D. A.; McMillan, F. M.; McNab, H.; Slawin, A. M. Z. AAA–DDD triple hydrogen bond complexes. *J. Am. Chem. Soc.* **2009**, *131*, 14116–14122.
- (18) Djurdjevic, S.; Leigh, D. A.; McNab, H.; Parsons, S.; Teobaldi, G.; Zerbetto, F. Extremely strong and readily accessible AAA–DDD triple hydrogen bond complexes. *J. Am. Chem. Soc.* **2007**, *129*, 476–477.

- (19) Murray, T. J.; Zimmerman, S. C. New triply hydrogen bonded complexes with highly variable stabilities. *J. Am. Chem. Soc.* **1992**, *114*, 4010–4011.
- (20) (a) Pappmeyer, M.; Vuilleumier, C. A.; Pavan, G. M.; Zhurov, K. O.; Severin, K. Molecularly defined nanostructures based on a novel AAA–DDD triple hydrogen bonding motif. *Angew. Chem., Int. Ed.* **2016**, *55*, 1685–1689. (b) Pappmeyer, M.; et al. Molecularly Defined Nanostructures Based on a Novel AAA–DDD Triple Hydrogen-Bonding Motif. *Angew. Chem.* **2016**, *128*, 1717–1721.
- (21) Zimmerman, S. C.; Murray, T. J. Hydrogen bonded complexes with the AA–DD, AA–DDD, and AAA–DD motifs: the role of three centered (bifurcated) hydrogen bonding. *Tetrahedron Lett.* **1994**, *35*, 4077–4080.
- (22) Prins, L. J.; Reinhoudt, D. N.; Timmerman, P. Noncovalent synthesis using hydrogen bonding. *Angew. Chem., Int. Ed.* **2001**, *40*, 2382–2426.
- (23) Backhouse, O. J.; Thacker, J. C. R.; Popelier, P. L. A. A re-evaluation of factors controlling the nature of complementary hydrogen-bonded networks. *Chem. Phys. Chem.* **2019**, *20*, 555–564.
- (24) van der Lubbe, S. C. C.; Fonseca Guerra, C. The nature of hydrogen bonds: a delineation of the role of different energy components on hydrogen bond strengths and lengths. *Chem. Asian J.* **2019**, *14*, 2760–2769.
- (25) van der Lubbe, S. C. C.; Zaccaria, F.; Sun, X.; Fonseca Guerra, C. Secondary electrostatic interaction model revised: prediction comes mainly from measuring charge accumulation in hydrogen-bonded monomers. *J. Am. Chem. Soc.* **2019**, *141*, 4878–4885.
- (26) Karas, L. J.; Wu, C.-H.; Das, R.; Wu, J. I.-C. Hydrogen bond design principles. *WIREs Comput. Mol. Sci.* **2020**, No. e1477.
- (27) Elgabarty, H.; Khaliullin, R. Z.; Kühne, T. D. Covalency of hydrogen bonds in liquid water can be probed by proton nuclear magnetic resonance experiments. *Nat. Commun.* **2015**, *6*, No. 8318.
- (28) Arunan, E.; Desiraju, G. R.; Klein, R. A.; Sadlej, J.; Scheiner, S.; Alkorta, I.; Clary, D. C.; Crabtree, R. H.; Dannenberg, J. J.; Hobza, P.; et al. Defining the hydrogen bond: an account (IUPAC technical report). *Pure Appl. Chem.* **2011**, *83*, 1619–1636.
- (29) Poater, J.; Fradera, X.; Solà, M.; Duran, M.; Simon, S. On the electron-pair nature of the hydrogen bond in the framework of the atoms in molecules theory. *Chem. Phys. Lett.* **2003**, *369*, 248–255.
- (30) van der Lubbe, S. C. C.; Fonseca Guerra, C. Hydrogen-bond strength of CC and GG pairs determined by steric repulsion: electrostatics and charge transfer overruled. *Chem. - Eur. J.* **2017**, *23*, 10249–10253.
- (31) Grosch, A. A.; van der Lubbe, S. C. C.; Fonseca Guerra, C. Nature of intramolecular resonance assisted hydrogen bonding in malonaldehyde and its saturated analogue. *J. Phys. Chem. A* **2018**, *122*, 1813–1820.
- (32) Guillaumes, L.; Simon, S.; Fonseca Guerra, C. The role of aromaticity, hybridization, electrostatics, and covalency in resonance assisted hydrogen bonds of adenine–thymine (AT) base pairs and their mimics. *ChemistryOpen* **2015**, *4*, 318–327.
- (33) Sanz, P.; Mó, O.; Yáñez, M.; Elguero, J. Resonance-assisted hydrogen bonds: a critical examination. structure and stability of the enols of β -diketones and β -enaminones. *J. Phys. Chem. A* **2007**, *111*, 3585–3591.
- (34) Gilli, G.; Bellucci, F.; Ferretti, V.; Bertolasi, V. Evidence for resonance-assisted hydrogen bonding from crystal-structure correlations on the enol form of the β -diketone fragment. *J. Am. Chem. Soc.* **1989**, *111*, 1023–1028.
- (35) Hoja, J.; Sax, A. F.; Szalewicz, K. Is electrostatics sufficient to describe hydrogen-bonding interactions? *Chem. - Eur. J.* **2014**, *20*, 2292–2300.
- (36) Fonseca Guerra, C.; Zijlstra, H.; Paragi, G.; Bickelhaupt, F. M. Telomere structure and stability: covalency in hydrogen bonds, not resonance assistance, causes cooperativity in guanine quartets. *Chem. - Eur. J.* **2011**, *17*, 12612–12622.
- (37) Mahadevi, A. S.; Sastry, G. N. Cooperativity in noncovalent interactions. *Chem. Rev.* **2016**, *116*, 2775–2825.
- (38) Kobko, N.; Paraskevas, L.; del Rio, E.; Dannenberg, J. J. Cooperativity in amide hydrogen bonding chains: implications for protein-folding models. *J. Am. Chem. Soc.* **2001**, *123*, 4348–4349.
- (39) Kar, T.; Scheiner, S. Comparison of cooperativity in CH \cdots O and OH \cdots O hydrogen bonds. *J. Phys. Chem. A* **2004**, *108*, 9161–9168.
- (40) Fonseca Guerra, C.; van der Wijst, T.; Bickelhaupt, F. M. Supramolecular switches based on the guanine–cytosine (GC) Watson–Crick pair: effect of neutral and ionic substituents. *Chem. - Eur. J.* **2006**, *12*, 3032–3042.
- (41) Gilli, G.; Gilli, P. Towards a unified hydrogen-bond theory. *J. Mol. Struct.* **2000**, *552*, 1–15.
- (42) Reynisson, J.; McDonald, E. Tuning of hydrogen bond strength using substituents on phenol and aniline: A possible ligand design strategy. *J. Comput. Aided Mol. Des.* **2004**, *18*, 421–431.
- (43) Mata, I.; Molins, E.; Alkorta, I.; Espinosa, E. Tuning the interaction energy of hydrogen bonds: the effect of the substituent. *J. Phys. Chem. A* **2011**, *115*, 12561–12571.
- (44) Pareras, G.; Palusiak, M.; Duran, M.; Solà, M.; Simon, S. Tuning the strength of the resonance-assisted hydrogen bond in *o*-hydroxybenzaldehyde by substitution in the aromatic ring. *J. Phys. Chem. A* **2018**, *122*, 2279–2287.
- (45) Vallejo Narváez, W. E.; Jiménez, E. I.; Cantú-Reyes, M.; Yatsimirsky, A. K.; Hernández-Rodríguez, M.; Rocha-Rinza, T. Stability of doubly and triply H-bonded complexes governed by acidity–basicity relationships. *Chem. Commun.* **2019**, *55*, 1556–1559.
- (46) Vallejo Narváez, W. E.; Jiménez, E. I.; Romero-Montalvo, E.; Sauza-de la Vega, A.; Quiroz-García, B.; Hernández-Rodríguez, M.; Rocha-Rinza, T. Acidity and basicity interplay in amide and imide self-association. *Chem. Sci.* **2018**, *9*, 4402–4413.
- (47) Beijer, F. H.; Sijbesma, R. P.; Vekemans, J. A. J. M.; Meijer, E. W.; Kooijman, H.; Spek, A. L. Hydrogen-bonded complexes of diaminopyridines and diaminotriazines: opposite effect of acylation on complex stabilities. *J. Org. Chem.* **1996**, *61*, 6371–6380.
- (48) Gooch, A.; McGhee, A. M.; Pellizzaro, M. L.; Lindsay, C. I.; Wilson, A. J. Substituent control over dimerization affinity of triply hydrogen bonded heterodimers. *Org. Lett.* **2011**, *13*, 240–243.
- (49) Chu, W.-J.; Chen, C.-F. Tunable conformation and stability of amidourea-based hydrogen-bonded heteroduplexes. *Tetrahedron* **2012**, *68*, 9200–9205.
- (50) Liu, R.; Cheng, S.; Baker, E. S.; Smith, R. D.; Zeng, X. C.; Gong, B. Surprising impact of remote groups on the folding–unfolding and dimer-chain equilibria of bifunctional H-bonding unimers. *Chem. Commun.* **2016**, *52*, 3773–3776.
- (51) *ADF2017, SCM, Theoretical Chemistry*, Vrije Universiteit: Amsterdam, The Netherlands, <http://www.scm.com>.
- (52) te Velde, G.; Bickelhaupt, F. M.; Baerends, E. J.; Fonseca Guerra, C.; van Gisbergen, S. J. A.; Snijders, J. G.; Ziegler, T. Chemistry with ADF. *J. Comput. Chem.* **2001**, *22*, 931–967.
- (53) Fonseca Guerra, C.; Snijders, J. G.; te Velde, G.; Baerends, E. J. Towards an order-N DFT method. *Theor. Chem. Acc.* **1998**, *99*, 391–403.
- (54) Grimme, S.; Antony, J.; Ehrlich, S.; Krieg, H. A consistent and accurate ab initio parametrization of density functional dispersion correction (DFT-D) for the 94 elements H–Pu. *J. Chem. Phys.* **2010**, *132*, No. 154104.
- (55) Johnson, E. R.; Becke, A. D. A post-Hartree–Fock model of intermolecular interactions. *J. Chem. Phys.* **2005**, *123*, No. 024101.
- (56) Lee, C.; Yang, W.; Parr, R. G. Development of the Colle–Salvetti correlation-energy formula into a functional of the electron density. *Phys. Rev. B* **1988**, *37*, 785–789.
- (57) Becke, A. D. Density-functional exchange-energy approximation with correct asymptotic behavior. *Phys. Rev. A* **1988**, *38*, 3098–3100.
- (58) Brauer, B.; Kesharwani, M. K.; Kozuch, S.; Martin, J. M. L. The S66x8 benchmark for noncovalent interactions revisited: explicitly correlated ab initio methods and density functional theory. *Phys. Chem. Chem. Phys.* **2016**, *18*, 20905–20925.

(59) Fonseca Guerra, C.; van der Wijst, T.; Poater, J.; Swart, M.; Bickelhaupt, F. M. Adenine versus guanine quartets in aqueous solution: dispersion-corrected DFT study on the differences in π -stacking and hydrogen-bonding behavior. *Theor. Chem. Acc.* **2010**, *125*, 245–252.

(60) Fonseca Guerra, C.; Bickelhaupt, F. M.; Snijders, J. G.; Baerends, E. J. Hydrogen bonding in DNA base pairs: reconciliation of theory and experiment. *J. Am. Chem. Soc.* **2000**, *122*, 4117–4128.

(61) Legault, C. Y. *CYLVIEW 1.0b*, Université de Sherbrooke: Sherbrooke, <http://www.cylview.org>; 2009.

(62) Fonseca Guerra, C.; Handgraaf, J.-W.; Baerends, E. J.; Bickelhaupt, F. M. Voronoi Deformation Density (VDD) Charges: Assessment of the Mulliken, Bader, Hirshfeld, Weinhold, and VDD Methods for Charge Analysis. *J. Comput. Chem.* **2004**, *25*, 189–210.

(63) Clayden, J.; Greeves, N.; Warren, S. *Organic Chemistry*, 2nd ed.; Oxford University Press: New York, 2012; pp 471–497.

(64) Stasyuk, O. A.; Szatyłowicz, H.; Krygowski, T. M.; Fonseca Guerra, C. How amino and nitro substituents direct electrophilic aromatic substitution in benzene: an explanation with Kohn–Sham molecular orbital theory and Voronoi deformation density analysis. *Phys. Chem. Chem. Phys.* **2016**, *18*, 11624–11633.